

Constraining Baryon–Dark Matter Scattering with the Cosmic Dawn 21-cm Signal

Anastasia Fialkov

Harvard-Smithsonian Center for Astrophysics, 60 Garden Street, Cambridge, MA 02138, USA

Rennan Barkana and Aviad Cohen

Raymond and Beverly Sackler School of Physics and Astronomy, Tel Aviv University, Tel Aviv 69978, Israel

(Dated: March 1, 2018)

The recent detection of an anomalously strong 21-cm signal of neutral hydrogen from Cosmic Dawn by the EDGES Low-Band radio experiment can be explained if cold dark matter particles scattered off the baryons draining excess energy from the gas. In this Letter we explore the expanded range of the 21-cm signal that is opened up by this interaction, varying the astrophysical parameters as well as the properties of dark matter particles in the widest possible range. We identify models consistent with current data by comparing to both the detection in the Low-Band and the upper limits from the EDGES High-Band antenna. We find that consistent models predict a 21-cm fluctuation during Cosmic Dawn that is between 3 and 30 times larger than the largest previously expected without dark matter scattering. The expected power spectrum exhibits strong Baryon Acoustic Oscillations imprinted by the velocity-dependent cross-section. The latter signature is a smoking gun of the velocity-dependent scattering and could be used by interferometers to verify the dark matter explanation of the EDGES detection.

Keywords: 21-cm signal, dark matter

Introduction: The first few hundred million years after the Big Bang are the least explored period in the history of the Universe. This epoch is marked by some of the most interesting events in cosmic history such as the formation of the very first stars and black holes. However, what makes this epoch even more attractive for observers and theorists alike is that dark matter might manifest itself differently than today in the unmatched physical conditions of the early Universe. Even though conventional dark matter models assume only gravitational interactions with ordinary baryonic matter, other forms of couplings, such as collisions between dark matter and gas, are not ruled out and could be important at early times when the density of matter was much higher than today. Such interactions could modify the thermal and ionization histories, leaving fingerprints in the 21-cm signal of atomic hydrogen [1–3].

In the standard cosmology, Compton scattering couples the baryon temperature, T_{gas} , to the temperature of the Cosmic Microwave Background (CMB) at redshifts above $z_{\text{dec}} \sim 200$. At lower redshifts, T_{gas} is expected to cool adiabatically due to the expansion of the Universe until the moment when the first X-ray sources turn on, injecting energy into the gas. Because dark matter is expected to decouple earlier and be much colder than the gas, collisions between baryons and dark matter particles could drain excess energy from the gas leading to its over-cooling [1], while the relative velocity between dark matter and the gas could in some cases result in overall over-heating of the baryons [2].

The 21-cm line of neutral atomic hydrogen with a rest-frame frequency of 1.42 GHz is one of the most promising probes of this epoch. This signal is sensitive to the thermal and ionization states of the baryons and, thus, can be

used to measure the energy balance of the early Universe. The brightness temperature of the 21-cm line, T_{21} , is coupled to the kinetic temperature of the baryons by two processes: During the cosmic Dark Ages ($35 \lesssim z \lesssim 1100$, the epoch preceding the formation of the very first stars) the gas is dense enough for interatomic collisions to drive the effective temperature of the 21-cm transition to the temperature of the gas, a process that becomes less efficient as the Universe expands. During the subsequent epoch of Cosmic Dawn ($15 \lesssim z \lesssim 35$) when the first stars are formed, the main driver is the Ly- α radiation produced by stars which couples the two temperatures via the Wouthuysen-Field process [4, 5]. Because gas is colder than the background CMB at $z < z_{\text{dec}}$ and before the first X-ray sources turn on, the 21-cm signal from the Dark Ages and Cosmic Dawn is seen in absorption against the CMB. Features of the high-redshift 21-cm signal depend on the underlying astrophysics [6], but also on the properties of dark matter particles, if the latter affect either the thermal or the ionization state of the gas [1–3]. Therefore, the 21-cm signal can be used as a unique probe of the dark sector.

Although exploration of the high-redshift domain is one of the most active areas of research in astrophysics, properties of the early Universe are still poorly constrained. The uncertainty in astrophysical parameters and the limited understanding of the dark matter physics propagate into the 21-cm modeling and result in a large variety of allowed signals. The dependence of the expected 21-cm signal on astrophysical parameters has been extensively explored [6–8]. It is the goal of this Letter to explore the 21-cm signal over the parameter space of both astro- and dark matter physics.

Observation and Theory: The first detection of the 21-

cm signal from Cosmic Dawn was recently reported by the Low-Band antenna of the Experiment to Detect the Global EoR Signature (EDGES) [9]. After removal of the foregrounds and the instrumental noise, excess signal was found in the data of the Low-Band antenna observing in the 50-100 MHz frequency band and probing the 21-cm signal from the redshift range of $z \approx 13.2 - 27.4$. The extracted cosmological signal, centered at $\nu = 78 \pm 2$ MHz (which corresponds to $z = 17.2$), features a broad absorption trough of $T_{21} = -500^{+200}_{-500}$ mK, where the error corresponds to 99% confidence including both thermal and systematic noise. In the standard cosmological scenario, the strongest possible absorption expected at $z \sim 17$ is -209 mK, which corresponds to a gas temperature of $T_{\text{gas}} \sim 7$ K. The observed $T_{21} < 300$ mK requires the gas to be much colder, $T_{\text{gas}} < 5.1$ K, which is hard to explain by astrophysics alone [3]. Feng & Holder [10] suggest that an excess radio background, such as seen by ARCADE 2 [11], could produce anomalously strong absorption in the 21-cm signal at $z \sim 20$. However, the ARCADE 2 excess alone does not require astrophysical explanation and can be explained by carefully modeling the galactic contribution [12].

To explain the anomalously strong absorption seen by EDGES Low, Barkana (2018) [3] invoked elastic velocity-dependent scattering between baryons and dark matter (b-DM scattering). The absorption trough as deep as detected by EDGES is obtained if baryons scatter off dark matter particles with masses in the range $m_\chi < 4.3$ GeV. The scattering cross-section is assumed to be velocity-dependent, $\sigma(v) = \sigma_1 (v/1\text{km s}^{-1})^{-n}$, where $\sigma_1 > 3.4 \times 10^{-21}$ cm² is the normalization assuming $n = 4$, and v is the relative velocity between the baryon and the dark matter particle. Even though the results are derived for $n = 4$ (a theory often considered in the literature and corresponding to a Coulomb-like b-DM scattering) the qualitative conclusion is more general and is not limited by the specific type of scattering. Astrophysics also plays an important role, as the deep absorption in the EDGES Low-Band is produced only in the presence of the stellar Ly- α background; the central frequency and the depth of the trough are determined, in addition to b-DM scattering, by the timing and intensity of both the Ly- α and the X-ray radiative backgrounds.

A major role is played by the remnant b-DM relative velocity v_{bdm} from the early universe [2, 3]. As a result of the velocity-dependent scattering, T_{21} is expected to be modulated by the velocity field: regions where the velocity is low cool stronger and exhibit a stronger absorption signal; while regions where the velocity is high cool less. Examples of this dependence are shown in Fig. 1 and the effect is discussed further in the text.

Cosmic Dawn Signal: We model the 21-cm signal as in [3] over the large parameter space of possible astrophysical and dark matter properties. To describe astrophysics we use seven free parameters (see ref. [8] for more de-

tails). Star formation is parameterized by two numbers: per-halo efficiency, $0.05\% \leq f_* \leq 50\%$, and minimum circular velocity (or, equivalently, the minimal cooling mass) of star forming halos, $4.2 \leq V_c \leq 76.5$ km s⁻¹. We use three parameters to describe the X-ray population. These include the slope and the low-energy cutoff ($-1.5 \leq \alpha \leq -1$, $0.1 \leq \nu_{\text{min}} \leq 3$ keV) of the spectral energy distribution, which is assumed to have a power law shape. The total X-ray luminosity is assumed to scale as the star formation rate and is parameterized by f_X with $10^{-4} \leq f_X \leq 1000$; $f_X = 1$ corresponds to the luminosity of low-redshift X-ray counterparts, with the redshift evolution of metallicity taken into account [13, 14]. The ionizing efficiency of sources (calibrated to produce the total CMB optical depth consistent with the Planck data [15]) and the mean free path of ionizing photons ($20 \leq R_{\text{mfp}} \leq 40$ comoving Mpc) are the other two free parameters. For the study presented here we use a compilation of 6389 different astrophysical models populating the entire parameter space. For each astrophysical scenario we ran 51 models to include the dark matter physics. The b-DM scattering adds two parameters: the mass of dark matter particles, $0.0032 < m_\chi < 100$ GeV, and the cross-section $10^{-30} < \sigma_1 < 3.16 \times 10^{-18}$ cm². The range of each of the parameters is consistent with existing observational limits [3].

In the absence of scattering, the 21-cm signal is calculated using a state-of-the-art semi-numerical code [6, 14]. Given a set of astrophysical parameters, the simulation generates histories of the 21-cm signal in comoving volumes of 384^3 Mpc³ resolved down to 3 comoving Mpc. On smaller scales sub-grid models are employed. Processes such as the growth of structure, star formation, heating and ionization are incorporated. In the calculation, large scale structure is tracked from $z \sim 60$, just after the first stars are expected to form in the observable Universe, down to $z \sim 6$ when neutral gas is completely reionized. The reionization history is calibrated to observations [15]. Stars and stellar remnants produce inhomogeneous X-ray, Ly- α , Lyman-Werner and ultraviolet radiative backgrounds. The impact of radiation on the environment is calculated, including heating of the intergalactic medium by X-rays.

The b-DM scattering changes the energy budget of the gas. To calculate the complete 21-cm signal we follow the approach taken by Barkana (2018) [3]. We calculate the gas temperature accounting for both the scattering term (as a function of the local value of relative velocity v_{bdm}) and the astrophysical heating rate. The 21-cm signal is then calculated using the corresponding stellar Ly- α and ionizing backgrounds. We calculate the global 21-cm signal (as observed by EDGES) averaging over the value of v_{bdm} which is drawn from the Maxwell-Boltzmann distribution. In addition to the globally-averaged signal we estimate the r.m.s. of its fluctuations from the Dark Ages and Cosmic Dawn. For the purpose of this Letter we ne-

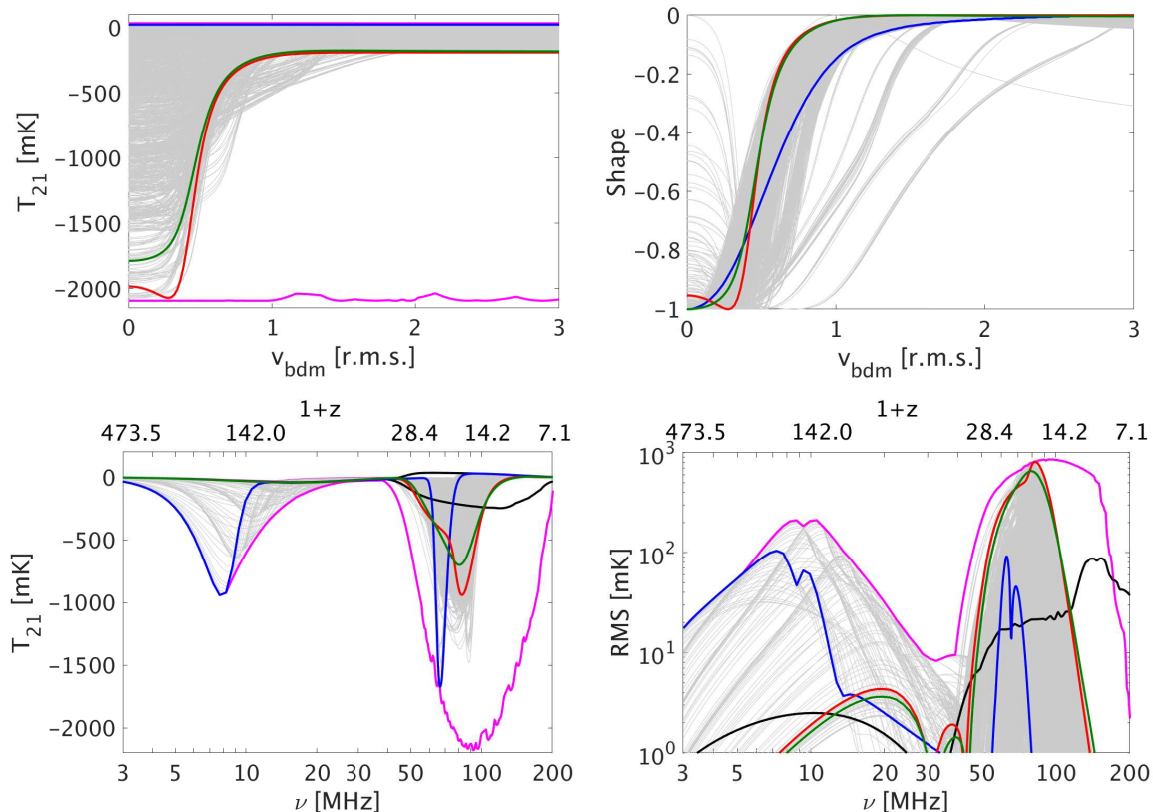


FIG. 1. **Top:** The function $T_{21}(v_{\text{bDM}})$ at $z = 17$ in units of mK (left) and its shape (right) versus the local relative baryon-DM velocity v_{bDM} in units of the r.m.s. velocity. To show the shape we re-scaled each curve along the y -axis so that it ranges from -1 to 0 . **Bottom:** Global (i.e., velocity-averaged) 21-cm signal (left) and r.m.s. of its fluctuations (right), as a function of frequency (bottom x -axis) or redshift (top x -axis). In every panel we show the envelope of all the possible signals without b-dm scattering (black, 6389 models) and with the scattering included (magenta, 325839 models). Also shown are all the models consistent with EDGES Low-Band and High-Band (grey lines, 3046 models in total). Out of the latter compilation we highlight three models: the model with the deepest absorption trough (blue) which is characterized by (see text) $V_c = 16.5$ [km s $^{-1}$], $f_* = 0.5\%$, $f_X = 10$, $\alpha = -1$, $\nu_{\text{min}} = 1$ [keV], $\tau = 0.0703$, $R_{\text{mfp}} = 20$ [Mpc], $m_\chi = 0.0032$ [GeV] and $\sigma_1 = 316 \times 10^{-20}$ [cm 2]; the lowest redshift of heating transition (green) with $V_c = 16.5$ [km s $^{-1}$], $f_* = 0.3\%$, $f_X = 0.0721$, $\alpha = -1$, $\nu_{\text{min}} = 1$ [keV], $\tau = 0.0702$, $R_{\text{mfp}} = 30$ [Mpc], $m_\chi = 0.1$ [GeV] and $\sigma_1 = 1 \times 10^{-20}$ [cm 2]; and the highest r.m.s. (red) with $V_c = 16.5$ [km s $^{-1}$], $f_* = 0.5\%$, $f_X = 0.01$, $\alpha = -1$, $\nu_{\text{min}} = 0.1$ [keV], $\tau = 0.0775$, $R_{\text{mfp}} = 20$ [Mpc], $m_\chi = 0.0032$ [GeV] and $\sigma_1 = 1 \times 10^{-20}$ [cm 2].

glect the 21-cm fluctuations due to the density and inhomogeneous astrophysical radiation fields, such as X-ray and Ly- α backgrounds, due to the much larger fluctuations induced by the velocity-dependent cross-section.

Results: Fig. 1 shows the range at redshift 17 of the global (sky-averaged) signal $T_{21}(z)$ and the r.m.s. of the fluctuations expected from the entirety of the considered models, with and without the contribution from b-DM scattering. The variation on the sky is determined by the brightness temperature as a function of the local v_{bDM} ; this function is also shown in the figure. First, to highlight the importance of the scattering process we show an envelope of the maximal and minimal $T_{21}(z)$ as well as the maximal r.m.s. of the fluctuations for the entire ensemble of the 6389 astrophysical cases without b-DM scattering (these do in-

clude the astrophysical fluctuation sources), and 325839 cases including the scattering. The recent detection by EDGES Low-Band [9] and the non-detection by EDGES High-Band [16] constrain the space of both astrophysical and dark matter parameters. Here we only verify a rough agreement with the data by imposing the following cuts based on published 99% or 3σ limits: The data collected by EDGES High-Band rules out models with large variations and implies $|T_{21}(100\text{MHz}) - T_{21}(150\text{MHz})| < 300$ mK [16]. EDGES Low-Band data give a positive detection and require the absorption feature to be deep, broad and localized within the band [9]. Within 99% confidence, the cosmological signal should satisfy (i) $300 \text{ mK} < \max[T_{21}(62 < \nu < 68)] - \min[T_{21}(71 < \nu < 85)] < 1000$ mK, and (ii) $300 \text{ mK} < \max[T_{21}(92 < \nu < 98)] - \min[T_{21}(71 < \nu < 85)] < 1000$

mK. There are 3046 models in total, all shown in Fig. 1 (grey curves), that satisfy both sets of conditions. Another global signal experiment, LEDA [17], reported 2σ limit of -890 mK on the amplitude of T_{21} at $z \sim 20$, which could also be used to rule out extreme cases of baryon over-cooling. However, here we rely only on the EDGES data which provides stronger constraints.

We first examine all the considered models with and without b-DM scattering. Unlike in the cases of negligible scattering in which the shape of the signal is universal and is described by an absorption trough followed in some cases by an emission feature [6], the added parameter space of dark matter models contributes to a larger variety of shapes (e.g., multiple wiggles during the Cosmic Dawn absorption) for both the global signal and the r.m.s. of the fluctuation. The effect of dark matter on the absorption trough itself can be very strong, leading to an order of magnitude increase in the amplitude. Specifically, the deepest possible absorption in the case with no scattering is $T_{21} = -247$ mK at 120 MHz, while with the scattering the absorption trough can reach $T_{21} = -2180$ mK at 92 MHz. Additionally, the fluctuations are enhanced with the peak power shifting from 87.7 mK at 153 MHz to 855 mK at 97 MHz. For the entire ensemble of models without b-DM scattering the most negative feature of the global signal during Cosmic Dawn and Reionization ($6 < z < 35$, $39.5 < \nu < 202$ MHz) is anywhere between -247.15 [mK] and -8.02 [mK] and is localized in the $9.1 < z < 35$ range ($39.5 < \nu < 140.6$ MHz); while in all the considered scenarios with b-DM scattering the maximal absorption is between -2179.2 [mK] and -2.1 [mK] and can be located anywhere within the $6 < z < 35$ range. The strongest fluctuations are expected to have an r.m.s. amplitude between 1.5 and 87.7 mK with the redshift of the peak power in the range $6.8 < z < 30$ ($45.8 < \nu < 182.1$ MHz) in the models without scattering, and the maximal r.m.s. during Cosmic Dawn ($\nu < 100$ MHz, $z > 13.2$) is 25.3 mK. With scattering the maximal fluctuation amplitude (due to b-DM scattering only) can be anywhere between 0 and 855.4 mK at $6.3 < z < 35$. Finally, with the scattering affecting the energy budget, gas can be heated either faster or slower depending on the detailed balance between baryons and the dark sector. Specifically, we find that the redshift of the heating transition, i.e., the moment at which the brightness temperature transitions from absorption to emission during Cosmic Dawn or Reionization, varies over a wider range when the scattering is included, and can be anywhere within $6 < z_h < 35$ compared to $6 < z_h < 30.3$ in the case of no scattering.

Adding the EDGES constraints restricts both the amplitude and the position of the absorption trough. Namely, the absorption feature of the compatible models can only be as deep as -1673 mK to -304 mK and must peak in the narrow redshift range $14.9 < z < 20.4$ ($66.3 < \nu < 89.3$ MHz). This deep absorption trough

should be readily accessible to other global experiments such as SARAS-2 [18, 19], LEDA [17, 20], and SCI-HI/PRIZM [21]. The absorption feature is a manifestation of the thermal history of the gas and can be used to constrain the temperature of the gas. To agree with the observations, the range of z_h is restricted to $8.7 < z_h < 17.4$. In other words, baryons cannot be significantly hotter than the CMB at $z \sim 17$ (the center of EDGES Low-Band) and should heat up considerably at $z \sim 9 - 13$. In addition, extremely low heating efficiency is ruled out by both EDGES High-Band [22] and SARAS-2 [18, 19]. Finally, the scenarios favored by EDGES yield fluctuations stronger by an order of magnitude than those previously predicted (assuming collisionless dark matter), with the peak r.m.s. between 8.07 mK and 807.3 mK found at $14.4 < z < 21.9$ ($62.0 < \nu < 92.2$ MHz). Such strong fluctuations are easily detectable by interferometric arrays such as HERA [23] and SKA [24]. Note that a strong 21-cm signal is also possible during the dark ages but it is expected to be at extremely low frequencies.

Another statistic that can be measured from images taken by 21-cm interferometers is the probability distribution function (PDF) of the 21-cm brightness temperature (relative to the mean global temperature). If the function $T_{21}(v_{\text{bDM}})$ is monotonic, then this function can essentially be read off an observed PDF (assuming that the 21-cm fluctuations are indeed dominated by b-DM scattering), since the PDF of v_{bDM} itself is known to be Maxwellian [25]; however, Fig. 1 shows that in some cases this function is non-monotonic, so reconstructing it from the 21-cm PDF will involve model-fitting.

BAO: The relative b-DM velocity is supersonic at recombination and, because of the coupling between baryons and photons prior to recombination, the velocity field bears a strong BAO signature [25]. In the absence of b-DM scattering, v_{bDM} can generate enhanced oscillations in the 21-cm signal by modulating star formation in primordial halos [26, 27]. With the b-DM scattering, as a result of the dependence of the cross-section on v_{bDM} , the BAO feature in the 21-cm signal is expected to be even stronger, acting as a smoking gun signature of b-DM scattering [3]. An enhanced BAO pattern in the 21-cm power spectrum detected by an interferometric array, such as HERA and SKA, would be a telltale signal of b-DM scattering and would verify the EDGES detection as well as its dark matter interpretation.

In Fig. 2 we demonstrate the BAO pattern seen in the power spectrum of the 21-cm power signal from redshift $z = 17$ (assuming that DM cooling dominates and other 21-cm fluctuations can be neglected). To calculate the power spectrum we generated a distribution of the velocity field in units of the r.m.s. velocity (e.g., see Fig. 1 of [3]) in a comoving volume of 1.536^3 Gpc³. Next, for each model we transformed the velocity cube to the 21-cm signal using the $v_{\text{bDM}} \rightarrow T_{21}$ mapping from Fig. 1 (top

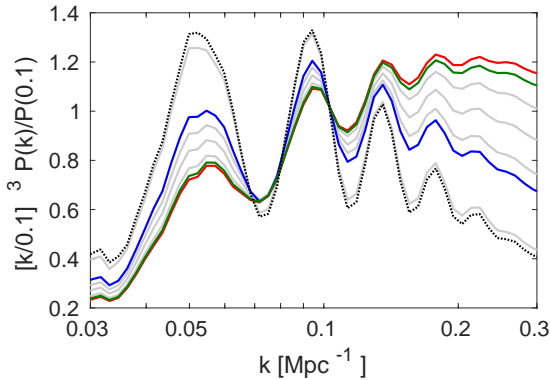


FIG. 2. Power spectrum of the 21-cm signal versus wavenumber at $z = 17$. The spectra are shown for the same highlighted models from Fig. 1: the model with the strongest absorption (blue), the lowest z_h (green) and the highest r.m.s. (red); in addition, several other random models from the ensemble compatible with EDGES are shown (grey). Also shown is the power spectrum of $v_{b,DM}$ (black dotted curve). The model with the strongest BAO has the following parameters: $V_c = 35.5$ [km s^{-1}], $f_* = 0.3\%$, $f_X = 0.0721$, $\alpha = -1.5$, $\nu_{min} = 0.4$ [keV], $\tau = 0.071$, $R_{mfp} = 30$ [Mpc], $m_\chi = 0.56$ [GeV] and $\sigma_1 = 4.6 \times 10^{-20}$ [cm^2]. In order to highlight the BAO shape, all the curves are normalized to unity at $k = 0.1$ [Mpc^{-1}].

row) and calculated the power spectrum. The resulting power spectra are shown in Fig. 2. To highlight the BAO shape (the r.m.s. amplitude was separately shown in Fig. 1) we show the power spectra relative to their value at $k = 0.1 \text{ Mpc}^{-1}$ and average over 10 independent realizations of the initial velocity cubes to compensate for the cosmic variance effect on the largest scales.

Conclusions: The recent detection by EDGES Low-Band, if indeed cosmological, requires a new theoretical explanation beyond the standard astrophysical model. In this Letter, considering b-DM scattering as a viable mechanism to produce the observed absorption, we have surveyed the resulting parameter space of astrophysical and dark matter properties. We have shown that the expected global signal and r.m.s. of the fluctuations vary over a much larger range than before. The velocity-dependent cross-section imprints enhanced BAOs which could be used to constrain dark matter theories.

[1] H. Tashiro, K. Kadota, and J. Silk, *PRD* **90**, 083522 (2014), arXiv:1408.2571.
[2] J. B. Muñoz, E. D. Kovetz, and Y. Ali-Haïmoud, *PRD* **92**, 083528 (2015), arXiv:1509.00029.
[3] R. Barkana, *Nature* 10.1038/nature25791.
[4] S. A. Wouthuysen, *AJ* **57**, 31 (1952).
[5] G. B. Field, *Proceedings of the IRE* **46**, 240 (1958).
[6] A. Cohen, A. Fialkov, R. Barkana, and M. Lotem,

MNRAS **472**, 1915 (2017), arXiv:1609.02312.
[7] A. Cohen, A. Fialkov, and R. Barkana, *ArXiv e-prints* (2017), arXiv:1709.02122.
[8] A. Cohen, A. Fialkov, R. Barkana, and R. A. Monsalve, in prep..
[9] J. D. Bowman, A. E. E. Rogers, R. A. Monsalve, T. J. Mozdzen, and N. Mahesh, *Nature* 10.1038/nature25792.
[10] C. Feng and G. Holder, *ArXiv e-prints* (2018), arXiv:1802.07432.
[11] D. J. Fixsen, A. Kogut, S. Levin, M. Limon, P. Lubin, P. Mirel, M. Seiffert, J. Singal, E. Wollack, T. Villela, and C. A. Wuensche, *ApJ* **734**, 5 (2011), arXiv:0901.0555.
[12] R. Subrahmanyan and R. Cowsik, *ApJ* **776**, 42 (2013), arXiv:1305.7060.
[13] T. Fragos, B. D. Lehmer, S. Naoz, A. Zezas, and A. Basu-Zych, *ApJL* **776**, L31 (2013), arXiv:1306.1405.
[14] A. Fialkov, R. Barkana, and E. Visbal, *Nature (London)* **506**, 197 (2014), arXiv:1402.0940.
[15] Planck Collaboration, P. A. R. Ade, N. Aghanim, M. Arnaud, M. Ashdown, J. Aumont, C. Baccigalupi, A. J. Banday, R. B. Barreiro, J. G. Bartlett, and et al., *AAP* **594**, A13 (2016), arXiv:1502.01589.
[16] R. A. Monsalve, A. E. E. Rogers, J. D. Bowman, and T. J. Mozdzen, *ApJ* **847**, 64 (2017), arXiv:1708.05817.
[17] G. Bernardi, J. T. L. Zwart, D. Price, L. J. Greenhill, A. Mesinger, J. Dowell, T. Eftekhari, S. W. Ellingson, J. Kocz, and F. Schinzel, *MNRAS* **461**, 2847 (2016), arXiv:1606.06006.
[18] S. Singh, R. Subrahmanyan, N. Udaya Shankar, M. Sathyanarayana Rao, A. Fialkov, A. Cohen, R. Barkana, B. S. Girish, A. Raghunathan, R. Somashekar, and K. S. Srivani, *ApJL* **845**, L12 (2017), arXiv:1703.06647.
[19] S. Singh, R. Subrahmanyan, N. Udaya Shankar, M. Sathyanarayana Rao, A. Fialkov, A. Cohen, R. Barkana, B. S. Girish, A. Raghunathan, R. Somashekar, and K. S. Srivani, *ArXiv e-prints* (2017), arXiv:1711.11281.
[20] D. C. Price, L. J. Greenhill, A. Fialkov, G. Bernardi, H. Garsden, B. R. Barsdell, J. Kocz, M. M. Anderson, S. A. Bourke, J. Craig, M. R. Dexter, J. Dowell, M. W. Eastwood, T. Eftekhari, S. W. Ellingson, G. Hallinan, J. M. Hartman, R. Kimberk, T. J. W. Lazio, S. Leiker, D. MacMahon, R. Monroe, F. Schinzel, G. B. Taylor, D. Werthimer, and D. P. Woody, *ArXiv e-prints* (2017), arXiv:1709.09313 [astro-ph.IM].
[21] T. C. Voytek, A. Natarajan, J. M. Jáuregui García, J. B. Peterson, and O. López-Cruz, *ApJL* **782**, L9 (2014), arXiv:1311.0014.
[22] R. A. Monsalve, A. Fialkov, A. Cohen, R. Barkana, and J. D. Bowman, in prep..
[23] D. R. DeBoer, A. R. Parsons, J. E. Aguirre, P. Alexander, Z. S. Ali, A. P. Beardsley, G. Bernardi, J. D. Bowman, R. F. Bradley, C. L. Carilli, C. Cheng, E. de Lera Acedo, J. S. Dillon, A. Ewall-Wice, G. Fadana, N. Fagnoni, R. Fritz, S. R. Furlanetto, B. Glendenning, B. Greig, J. Grobbelaar, B. J. Hazelton, J. N. Hewitt, J. Hickish, D. C. Jacobs, A. Julius, M. Kariseb, S. A. Kohn, T. Lekalake, A. Liu, A. Loots, D. MacMahon, L. Malan, C. Malgas, M. Maree, Z. Martinot, N. Mathison, E. Matsetela, A. Mesinger, M. F. Morales, A. R. Neben, N. Patra, S. Pieterse, J. C. Pober, N. Razavi-Ghods, J. Ringuette, J. Robnett, K. Rosie, R. Sell, C. Smith,

- A. Syce, M. Tegmark, N. Thyagarajan, P. K. G. Williams, and H. Zheng, *PASP* **129**, 045001 (2017), arXiv:1606.07473 [astro-ph.IM].
- [24] L. Koopmans, J. Pritchard, G. Mellema, J. Aguirre, K. Ahn, R. Barkana, I. van Bemmell, G. Bernardi, A. Bonaldi, F. Briggs, A. G. de Bruyn, T. C. Chang, E. Chapman, X. Chen, B. Ciardi, P. Dayal, A. Ferrara, A. Fialkov, F. Fiore, K. Ichiki, I. T. Illiev, S. Inoue, V. Jelic, M. Jones, J. Lazio, U. Maio, S. Majumdar, K. J. Mack, A. Mesinger, M. F. Morales, A. Parsons, U. L. Pen, M. Santos, R. Schneider, B. Semelin, R. S. de Souza, R. Subrahmanyan, T. Takeuchi, H. Vedantham, J. Wagg, R. Webster, S. Wyithe, K. K. Datta, and C. Trott, *Advancing Astrophysics with the Square Kilometre Array (AASKA14)*, 1 (2015), arXiv:1505.07568.
- [25] D. Tseliakhovich and C. Hirata, *Phys. Rev. D* **82**, 083520 (2010), arXiv:1005.2416.
- [26] N. Dalal, U.-L. Pen, and U. Seljak, *JCAP* **11**, 007 (2010), arXiv:1009.4704 [astro-ph.CO].
- [27] E. Visbal, R. Barkana, A. Fialkov, D. Tseliakhovich, and C. M. Hirata, *Nature* **487**, 70 (2012), arXiv:1201.1005.